Available online at www.sciencedirect.com
ScienceDirect
Journal of Molecular Graphics and Modelling 26 (2007) 401–408
Journal of Molecular Graphics and Modelling
www.elsevier.com/locate/JMGM

A quantum chemical study of the mechanism of action of Vitamin K epoxide reductase (VKOR) II. Transition states ☆

Charles H. Davis [a], David Deerfield II [b], Troy Wymore [b], Darrel W. Stafford [c], Lee G. Pedersen [d,e,*]

[a] Department of Biochemistry and Biophysics, UNC-CH, Chapel Hill, NC 27599, United States
[b] Pittsburgh Supercomputing Center, Biomedical Group, Pittsburgh, PA 15213, United States
[c] Department of Biology, UNC-CH, Chapel Hill, NC 27599, United States
[d] Laboratory of Structural Biology, NIEHS, Research Triangle Park, NC 27009, United States
[e] Department of Chemistry, UNC-CH, Chapel Hill, NC 27599, United States

Received 13 June 2006; accepted 24 October 2006
Available online 6 November 2006

Abstract

A reaction path including transition states is generated for the Silverman mechanism [R.B. Silverman, Chemical model studies for the mechanism of Vitamin K epoxide reductase, J. Am. Chem. Soc. 103 (1981) 5939–5941] of action for Vitamin K epoxide reductase (VKOR) using quantum mechanical methods (B3LYP/6-311G**). VKOR, an essential enzyme in mammalian systems, acts to convert Vitamin K epoxide, formed by Vitamin K carboxylase, to its (initial) quinone form for cellular reuse. This study elaborates on a prior work that focused on the thermodynamics of VKOR [D.W. Deerfield II, C.H. Davis, T. Wymore, D.W. Stafford, L.G. Pedersen, Int. J. Quant. Chem. 106 (2006) 2944–2952]. The geometries of proposed model intermediates and transition states in the mechanism are energy optimized. We find that once a key disulfide bond is broken, the reaction proceeds largely downhill. An important step in the conversion of the epoxide back to the quinone form involves initial protonation of the epoxide oxygen. We find that the source of this proton is likely a free mercapto group rather than a water molecule. The results are consistent with the current view that the widely used drug Warfarin likely acts by blocking binding of Vitamin K at the VKOR active site and thereby effectively blocking the initiating step. These results will be useful for designing more complete QM/MM studies of the enzymatic pathway once three-dimensional structural data is determined and available for VKOR.

Keywords: Vitamin K; VKOR; Reductase; Mechanisms; Transition states

1. Introduction

When the human vascular system is compromised, an exquisite sequence of reactions is catalyzed in response to the assault, with the immediate goal being the formation of a blood clot to re-seal the damaged system. A number of the enzymes that participate in the response system depend on the presence of Vitamin K for the post-translational modifications that render them active [1].

The main role of Vitamin K, an essential component of human physiology, is to provide for the conversion of glutamic acid (Glu) to gamma-carboxyglutamic acid (Gla). This post-translational modification occurs for some Glu residues that reside in the membrane-binding domain of several critical blood coagulation proteins. It is currently believed that the three forms of Vitamin K – Vitamin K, Vitamin K epoxide and Vitamin K hydroquinone – are involved in a catalytic cycle (Fig. 1).

Although Vitamin K was discovered in 1934 [2], it was only in the mid 1980s when the general details of the mechanism began to be unraveled [3]. Recently, the two key enzymes in the

☆ This paper was presented in the Goldstein symposium and is dedicated to the memory of Professor Jacob Goldstein.

* Corresponding author at: Department of Chemistry, UNC-CH, Chapel Hill, NC 27599, United States. Tel.: +1 919 962 1578; fax: +1 919 962 2388.
E-mail address: Lee_Pedersen@unc.edu (L.G. Pedersen).

1093-3263/$ – see front matter © 2006 Elsevier Inc. All rights reserved.
doi:10.1016/j.jmgm.2006.10.005

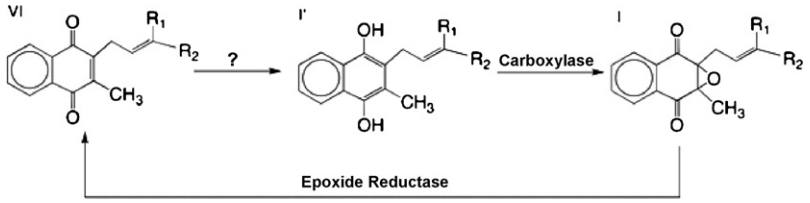

Fig. 1. The Vitamin K catalytic cycle. The result of the carboxylase activity is to convert Glu to Gla in a number of sites in Vitamin K-dependent proteins. The enzyme for the initial reduction (? in the figure) is not known. Structure I is Vitamin K epoxide, structure I′ is Vitamin K hydroquinone and structure VI is Vitamin K.

catalytic cycle, the Vitamin K carboxylase [4] and the Vitamin K epoxide reductase [5,6] (VKOR) have been identified, sequenced and cloned. The identity of the reducing enzymatic species for (VI → I′, Fig. 1) is still an open question. A pertinent News and Views column in Nature [7] summarizes our knowledge to the present.

The drug Warfarin is the most studied inhibitor of the reductase, VKOR. The design of this agent was based on an isolate from fermented sweet clover, a deadly poison to livestock [8,9]. Over 7 million prescriptions of this drug were written for US patients in the year 2003 [10]. One of the interesting outcomes of the human genome project has been the quantitative details necessary to understand why all patients treated with drugs such as Warfarin do not respond the same way, i.e., there is considerable variability in the human phenotype. This situation leads to the danger of over/under prescribing Warfarin for any given individual. For instance, it has been shown recently that there are a significant number of single nucleotide polymorphisms for VKOR [11], which is the target of Warfarin, and at least one significant polymorphism for the cytochrome P450 gene 2C9 that metabolizes Warfarin [12]. The desire to ultimately be able to treat patients with knowledge-based enzyme reactivity along with genetic profile information drives the current work.

In this work, we will focus on the epoxide reductase. The significant studies of Dowd et al. [13,14], Silverman [15,16], Goodstadt and Ponting [17] and others, have made it possible to establish a (pseudo-enzymatic) mechanism by which the essential epoxide reductase activity may be modeled. The sequence of reactions proposed by Silverman [15] has been modified by practical consideration:

$$\mathrm{Ii} + \mathrm{H_2O} + \mathrm{HSCH_3} + {}^{-}\mathrm{SCH_3} \rightarrow \mathrm{Ia}$$

$$\mathrm{Ia} \rightarrow \mathrm{TS1} \rightarrow \mathrm{Ib}$$

$$\mathrm{Ib} \rightarrow \mathrm{IVi} + {}^{-}\mathrm{SCH_3} + \mathrm{H_2O}$$

$$\mathrm{IVi} + \mathrm{H^+} \rightarrow \mathrm{Vi}$$

$$\mathrm{Vi} + {}^{-}\mathrm{SCH_3} + \mathrm{H_2O} \rightarrow \mathrm{Va}$$

$$\mathrm{Va} \rightarrow \mathrm{TS2} \rightarrow \mathrm{Vb}$$

$$\mathrm{Vb} \rightarrow \mathrm{VI} + \mathrm{CH_3SSCH_3} + 2\mathrm{H_2O}$$

$$\text{Net}: \mathrm{Ii} + \mathrm{HSCH_3} + {}^{-}\mathrm{SCH_3} + \mathrm{H^+} \rightarrow \mathrm{VI} + \mathrm{CH_3SSCH_3} + \mathrm{H_2O}$$

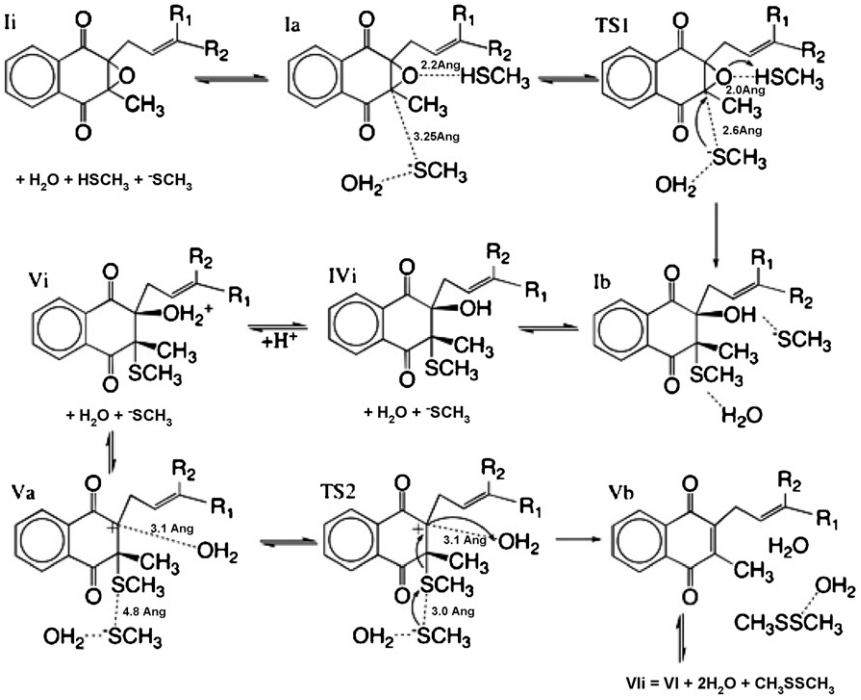

Fig. 2. A thiol/disulfide-based mechanism to reduce the Vitamin K epoxide to the quinone. This is a modification of the Silverman mechanism [15].

The mechanism could reasonably involve structures I–VI (Figs. 1 and 2). In this mechanicm, Vitamin K epoxide is reduced to the quinone form by sequential protonation, cysteine attack with loss of proton and rearrangement, protonation, attack by a second cysteine and finally, loss of a water and reductive elimination.

To date, no three-dimensional structures of the Vitamin K-carboxylase or epoxide reductase have been determined/published. With such structures, we would be able to design a QM/MM study to understand the enzymatic catalysis pathway. But, even if three-dimensional structures of the enzymes were available, it would be necessary to initially explore simple pseudo-enzymatic pathways to properly initiate QM/MM procedures. Since accurate quantum mechanical methods can now be applied reliably to systems the size of Vitamin K [18], we recently investigated the thermodynamics of the several pathways proposed with simple model substances [19]. We have now been able to elaborate on the pathway that is most similar to the original proposal of Silverman [15]. We have been able to locate several transition states as well as verify that a likely protonation source for breaking down the epoxide is a free mercapto group.

2. Methodology

All structures were fully geometry optimized using Gaussian 2003 implementation of density functional theory code [20]. The method/basis employed was B3LYP/6-311G** [21,22]. All non-transition structures were verified to be geometry minima by performing quadratic potential frequency calculations and examining the frequency list for imaginary values. By computing the frequencies of the transition state structures, it was also shown that the transition state is characterized by one imaginary frequency (negative force constant). These are relatively large, complex systems and finding the transition states proved challenging. The auxiliary suite of programs called GaussView [23] proved essential for following all details of the work. A procedure for finding the transition states was subsequently developed and it is included in an Appendix A. We hope this procedure will be of general use to others. The method/basis chosen has proven previously to be useful for exploring reactive intermediates [24,25]. From practical considerations of the computer resource requirements, balanced with the chemical importance of the extended side chain, the lengthy hydrophobic side chain of the Vitamin K analogs is truncated after the first double bond.

3. Results and discussion

3.1. $HSCH_3$ as source of protonation of epoxide

What is the source for the electrons that effect the reduction of Vitamin K epoxide (Fig. 1) by VKOR? Current thinking is based on the experimental finding that the enzymatic activity of VKOR is dependent on thiol reagents [26], a process whereby an active site disulfide is reduced to sulfhydryls with subsequent nucleophilic attack on the Vitamin K epoxide. Goodstadt and Ponting have shown [17] that the VKORC1 subdomains of VKORs occur in vertebrates, drosophila, plants, bacteria and archea. This VKORC1 domain possesses epoxide reduction capability. The active site residues [17] appear to be four cysteines and a Ser/Thr. Since the VKORC1 domain has been identified in some plants and bacteria fused to thioredoxin-like domains (thioredoxins are also oxioreductases), and since both VKORC1 and thioredoxins contain CXXC motifs (C = Cys = cysteine) that are structurally linked, the picture that emerges is that cysteines of the reductase are involved. The field is poised for the introduction of experimental three-dimensional data; such will have decisive impact. In the meantime, however, by application of information-based algorithms, it has recently been predicted that the key CXXC motif of VKOR is located in the third of three postulated transmembrane domains [27]. A transmembrane presence could make structure determination difficult. Significantly, it has also been shown that C132A or C135A mutations in the CXXC motif [28] abolish VKOR activity in the rat VKOR enzyme, which is highly homologous to human VKOR. It is possible that the disulfide bond breakage that initiates the Silverman mechanism involves these particular Cys residues, which may link through a disulfide bond.

Whereas our ultimate goal is to understand the enzymatic biochemistry, we can initiate the study by computing model

Table 1a
Energies computed for the proposed reductase mechanism[a,b]

Structure	E (au)	G°_{298} (au)
Ii	−1719.8845260	−1719.663254
Ia	−1719.9435007	−1719.677231
TS1-$HSCH_3$[c]	−1719.9280009	−1719.658816
Ib	−1719.9730805	−1719.692795
Ivi	−1719.9140800	−1719.666399
Vi	−1720.2401860	−1719.980817
Va	−1720.4152982	−1720.133945
TS2	−1720.4063427	−1720.120513
Vb	−1720.5281211	−1720.244224
VIi(1)	−1720.4987490	−1720.265621
VIi(2)	−1720.4997060	−1720.266268

[a] Definitions Ii = I + H_2O + $HSCH_3$ + $^{-}SCH_3$; IVi = IV + $^{-}SCH_3$ + H_2O; Vi = V + $^{-}SCH_3$ + H_2O; VIi = VI + CH_3SSCH_3 + 2H_2O.

[b] The terms ending with (A)i refer to the complex with infinite spacing between all reactants or products. The terms ending with (A)a refer to the reactants in their lowest energy optimized state in the enzymatic "pocket". The terms ending with (A)b refer to the products in their lowest energy optimized state in the enzymatic "pocket".

[c] TS1-$HSCH_3$ refers to TS1 with $HSCH_3$ as the epoxide stabilizing group.

Table 1b
Energies and free energies of other significant structures [17]

Structure	E (au)	G°_{298} (au)
I	−766.528279	−766.345558
IV	−1205.300452	−1205.069691
V	−1205.626558	−1205.384109
VI	−691.3203198	−691.14091
$HSCH_3$	−438.7426188	−438.720988
$^{-}SCH_3$	−438.1661801	−438.152939
H_2O	−76.44744792	−76.443769
CH_3SSCH_3	−876.2844902	−876.23782

(pseudo-enzymatic) pathways, which perhaps capture the spirit of the enzymatic chemistry. We have established a reasonable mechanism based on the Silverman proposal [15] to model the activity of VKOR (Fig. 2). There are 10 species, including 2 transition states. The energies and free energies (corrected to 298 K) of these species are given in Table 1a. The coordinates of the optimized structures are given in Supplementary Information. Previously determined [19] energies that are needed for the analysis given in this paper are listed in Table 1b. Table 2 gives the energy differences for the steps of the proposed mechanism.

The final optimized structures are shown in Fig. 3. The free energies as a function of reaction path step are shown in Fig. 4. We will consider each conversion step along the proposed mechanism pathway (Fig. 2):

- Step 1: Ii → Ia. *Ii*. The initial Vitamin K form is the epoxide. A water molecule, a methyl mercaptan and a de-protonated methyl mercaptan are located at infinite separation. It is essential to recognize that we do not know the details of how the disulfide bond gets broken. Most evidence so far points to the existence of a disulfide bond linking Cys 132–135. In the Silverman hypothesis, this disulfide is broken to provide a $–CH_2SH$ and a $–CH_2S^-$. This is where we begin.

  Ia. This form results from finding reasonable equilibrium positions (full optimization) for the components of the reaction. This form resides almost 9 kcal/mol in energy below the form at infinite separation. It is useful to consider the Vitamin K form to be ''in the enzyme pocket''.
- Step 2: I → TS1. *TS1*. A transition state (1 negative force constant) is found by first scanning the distance between the incoming $^-SCH_3$ and the epoxide carbon with the attached $–CH_3$. The procedure in Appendix A is then applied to the structure at the maximum energy along the scan path. The transition state found is about 11.5 kcal/mol above Ia and 2.8 kcal/mol above Ii.
- Step 3. TS1 → Ib. *Ib*. Structure 1b results from the transfer of a proton from the donor CH_3SH to the epoxide oxygen and the formation of the $C–SCH_3$ bond. The epoxide is now broken. This structure is more than 21 kcal/mol below TS1.

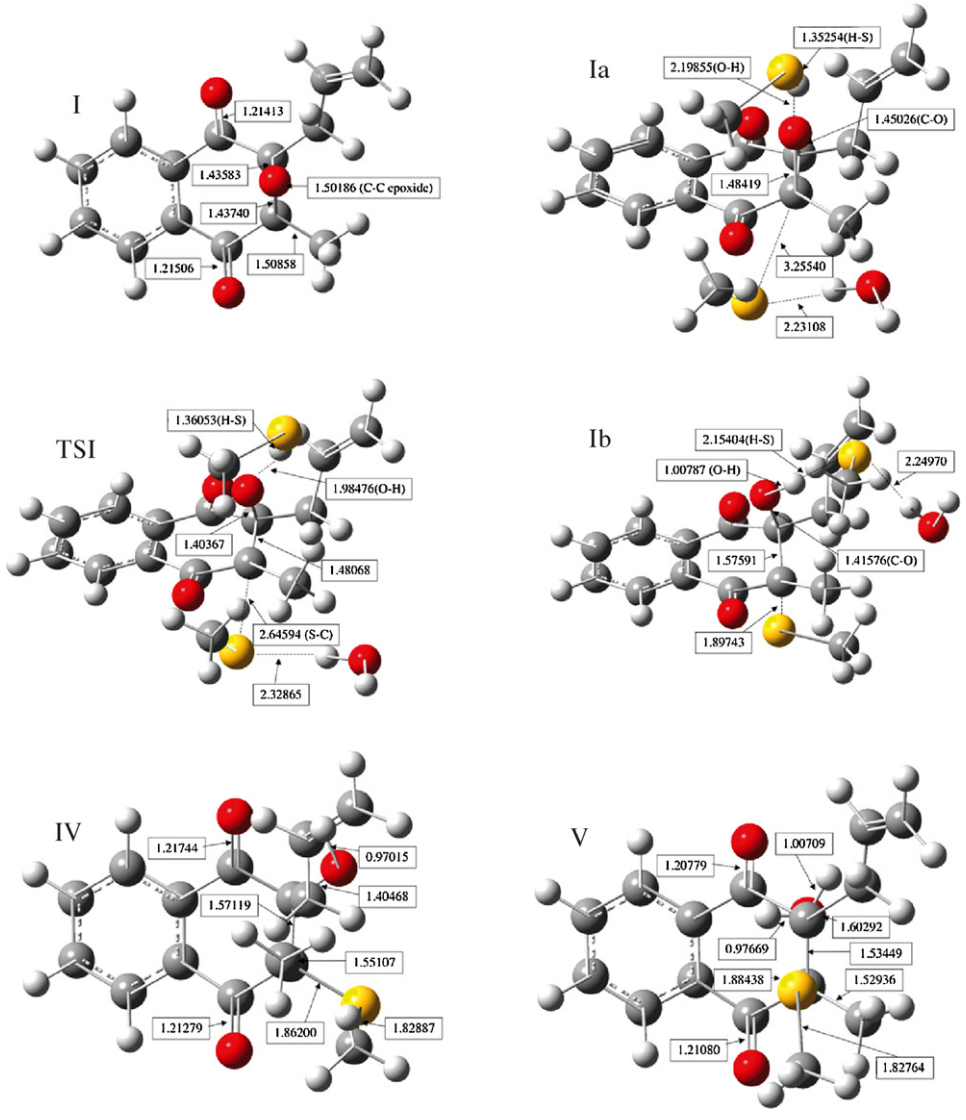

Fig. 3. Fully energy-optimized geometries (B3LYP/6-311G**) of species studied. Labels refer to nomenclature presented in Fig. 2.

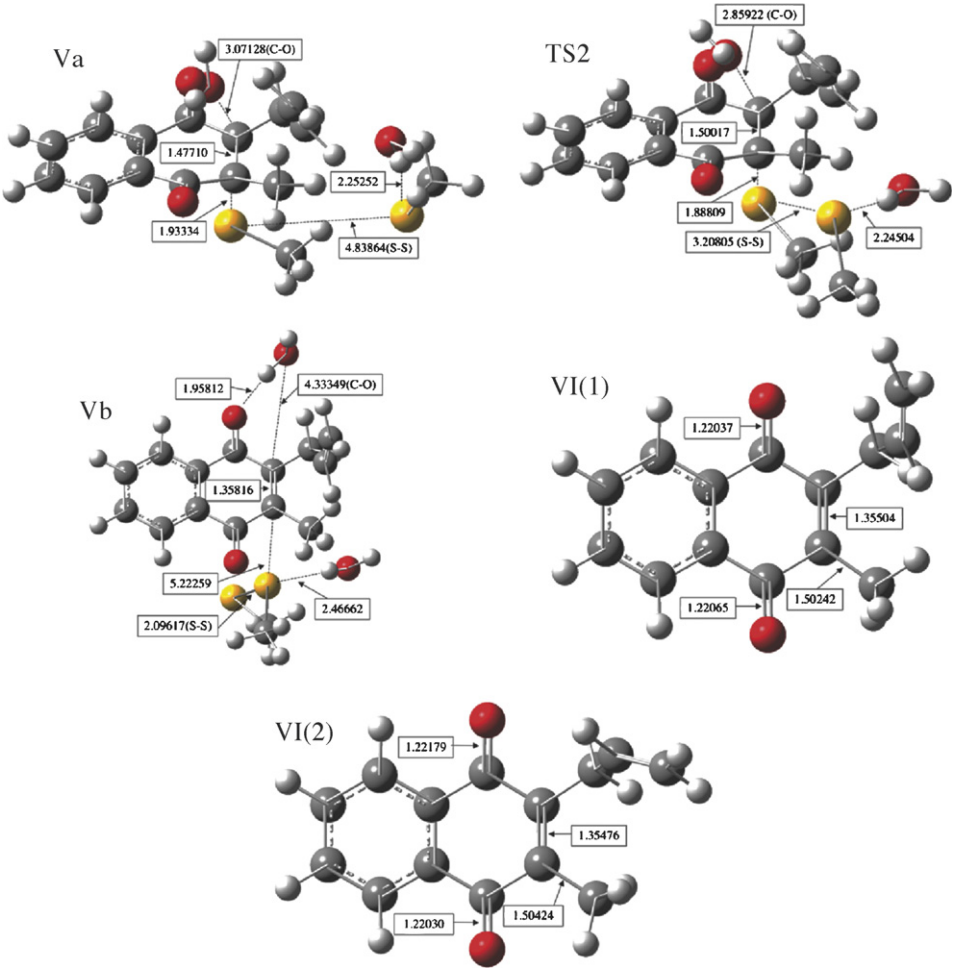

Fig. 3. (*Continued*).

- Step 4. Ib → IVi. *IVi*. The goal of the second portion of the mechanism is to remove the $^{-}SCH_3$ unit from the second ring of the Vitamin K intermediate. To accomplish this, it was necessary (because of the reactivity of the CH_2 of the side chain to an attacking $^{-}SCH_3$ two steps later) to rotate the R_1–R_2 side-chain and to "remove" the Vitamin K intermediate from the "enzyme pocket". This species is about 17 kcal/mol above the form Ib, most of this energy is the loss of the weak bonds of the $^{-}SCH_3$ and the H_2O molecule to the Vitamin K intermediate.
- Step 5. IVi → Vi. *Vi*. Structure IVi is protonated on the epoxide oxygen by an unknown source with a large drop in the energy (−197 kcal/mol). This step is also conducted "outside enzyme pocket", again to minimize undesirable side reactions as in the previous step.

Table 2
Energies and free energies for steps of the proposed reaction

Transition	ΔE (au)	ΔG°_{298} (au)	ΔE (kcal/mol)	ΔG°_{298} (kcal/mol)
Ii to Ia	−0.0589747	−0.0139770	−37.00662425	−8.7705675
Ia to TS1	0.0154998	0.0184150	9.7261496	11.5554125
TS1 to Ib	−0.0450796	−0.0339790	−28.28745527	−21.3218225
Ib to IVi	0.0590005	0.0263960	37.02279493	16.56349
IVi to Vi	−0.3261060	−0.3144180	−204.631515	−197.297295
Vi to Va	−0.1751122	−0.1531280	−109.8829181	−96.08782
Va to TS2	0.0089555	0.0134320	5.619582525	8.42858
TS2 to Vb	−0.1217784	−0.1237110	−76.41592717	−77.6286525
Vb to VIi(1)[a]	0.0293721	−0.0213970	18.4309802	−13.4266175
VIi(1) to VIi(2)[b]	−0.000957	−0.000647	−0.6005175	−0.4059925[c]

[a] VI(1) is structure VI with the rotated R group as used in transition state 2.
[b] VI(2) is structure VI with the R group not rotated (same arrangement as in I).
[c] ΔG°_{Total} = −378.3913 kcal/mol.

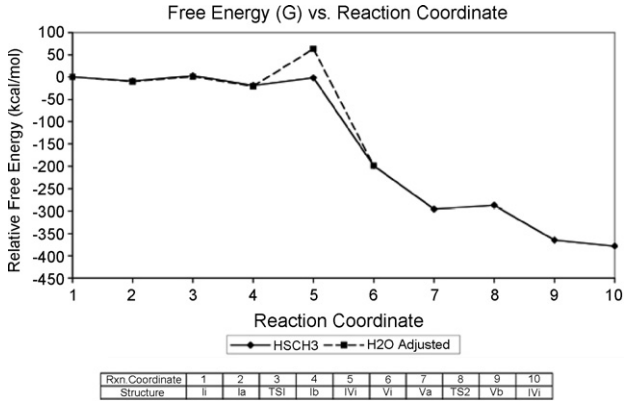

Fig. 4. Relative free energies for steps along the proposed mechanism (Fig. 2) with respect to initial structure, Ii. The labels for the species at each step are coordinated in the footnote. The solid line is for the mechanism using CH_3SH as the protonation source for the epoxide oxygen. The dashed line is for the mechanism using H_2O as the source of the proton.

- Step 6. Vi → Va. *Va*. We were able to find a stable species of IV, H_2O and $^{-}SCH_3$ back inside the "pocket". Note that this species is equivalent to protonation of the epoxide oxygen in structure Ib taken in concert with rotation of the R_1, R_2 side chain, translocation of the negatively charged $^{-}SCH_3$ entity with the associated water of Ib to an equilibrium and initial position of attack on the $^{-}SCH_3$ unit that is covalently bound to the Vitamin K intermediate. Restoration of the [water ($^{-}SCH_3$)] unit back into the "pocket" lowers the free energy by 96 kcal/mol. The sum of the free energies of steps 4, 5, and 6 is −285 kcal/mol.
- Step 7. Va → TS2. *TS2*. This species is the transition state for the breaking of the C–SCH3 bond and the forming of the –S–S-bond. This is a low energy barrier of +8 kcal/mol above the Va species free energy.
- Step 8. TS2 → Vb. *Vb*. This is almost the final state for the restored quinone. Two water molecules and the dimethyl disulfide are nearby still loosely interacting with VI. This form is almost 78 kcal/mole lower in free energy than the TS2 structure.
- Step 9. Vb → VI + $2H_2O$ + CH_3SSCH_3. This final step of the process takes the quinone product from the reaction "pocket" by removing the product water molecules and the disulfide to infinity. This step has a free energy gain of almost 14 kcal/mol with the concomitant entropy production of the products relative to the constrained reactants being the dominant contribution to the free energy.

The overall computed free energy path for the proposed mechanism (Fig. 2) is displayed in Fig. 4. The overall free energy for converting I → VI (epoxide to quinone) by the net reaction:

$$\mathrm{Ii} + \mathrm{HSCH_3} + {}^{-}\mathrm{SCH_3} + \mathrm{H^+} \rightarrow \mathrm{VI} + \mathrm{CH_3SSCH_3} + \mathrm{H_2O}$$

is −378.39 kcal/mol. This number is somewhat more exoergic than that found in our preliminary study of the thermodynamics of the epoxide → quinone process. In the current scheme, we have modified the previous mechanism so as to currently assume the starting existence of the $^{-}SCH_3$ species, which accounts for the overall difference.

3.2. H_2O as the source of the protonation of the epoxide

It is reasonable to consider H_2O as the source of the proton at the TS1 step. To test this possibility, it is necessary to substitute H_2O for $HSCH_3$ in the mechanism at the Ii (initial step). We can then superimpose the free energies of Ii for both the H_2O and the $HSCH_3$ paths. Using this reference, we can then compute the energies of the Ia, TS1, Ib, and IVi intermediates (Table 3 contains the energies of the additional geometry optimized structures needed to carry out this analysis).

After species IVi, the reaction is steeply downhill for the $HSCH_3$ case and would be expected to also be the case for the H_2O protonation. It is at the location of the IVi species that we see the largest relative difference (Fig. 4): the H_2O path costs 84 kcal/mol to go from Ib to IVi, whereas this cost is much lower (16.6 kcal/mol) for the $HSCH_3$ case.

3.3. No protonation source for the epoxide

A final consideration is having no source for protonation of the epoxide (equivalent to dropping $HSCH_3$ from the Ii, Ia, TS1

Table 3
(a) Energies of species with CH_3SH replaced by H_2O and (b) the Ii energies for the Ii case with CH_3SH and H_2O are superimposed and the energies and free energies for the steps of the H_2O reaction are given (dashed line in Fig. 4)

Structure	E (au)	G°_{298} (au)
(a) Energies of species with CH_3SH		
Ii	−1357.5893549	−1357.386035
Ia	−1357.6565130	−1357.401884
TS1-H_2O	−1357.6412488	−1357.385316
Ib	−1357.6783757	−1357.419092
IVi	−1357.5112834	−1357.285167

Transition	ΔE (au)	ΔG°_{298} (au)	ΔE (kcal/mol)	ΔG°_{298} (kcal/mol)
(b) The Ii energies for the Ii case with CH_3SH and H_2O				
Ii to Ia	−0.0671581	−42.14171026	−0.0158490	−9.9452475
Ia to TS1	0.0152642	9.578291775	0.0165680	10.39642
TS1 to Ib	−0.0371269	−23.29712975	−0.0337760	−21.19444
Ib to IVi	0.1670923	104.8504427	0.1339250	84.0379375

Table 4
(a) Energies of additional species necessary when there is no agent present to transfer a proton to the epoxide oxygen and (b) path differences in energy with the energies references to species Ii as in Table 3

Structure	E (au)	G°_{298} (au)
(a) Energies of additional species		
Ii	−1281.1419070	−1280.942266
Ia	−1281.1908330	−1280.956567
TS1-H_2O	−1281.1717716	−1280.939994
Ib	−1281.1876458	−1280.954063

Transition	ΔE (au)	ΔG°_{298} (au)	ΔE (kcal/mol)	ΔG°_{298} (kcal/mol)
(b) Path differences in energy				
Ii to Ia	−0.0489260	−30.70105151	−0.0143010	−8.9738775
Ia to TS1	0.0190614	11.96102222	0.0165730	10.3995575
TS1 to Ib	−0.0158742	−9.961079325	−0.0140690	−8.8282975

and Ib species). This necessitates computing the structures and energies of additional species (energy values shown in Table 4). Then, as before, we superimpose the energies for the Ii species and then compute differences along the reaction path. The free energies differences of the first two steps of the mechanism via all three cases (CH_3SH, H_2O, nothing) are similar; the difference for the third step in the "nothing case" is less stabilizing by about 12 kcal/mol. And the mechanism for this last case dies at the Ib species because for this case there is no proton to transfer to the epoxide oxygen.

4. Conclusions

We have computed the energies and geometries for the possible intermediates and transition states for the reduction of the Vitamin K epoxide back to the Vitamin K quinone form. The overall mechanism conforms as closely as possible to that proposed by Silverman in 1981 [15]. Since we do not have three-dimensional structural information on the reduction enzyme, we model the key (proposed) Cys residues in the mechanism as CH_3SH and the corresponding disulfide as CH_3SSCH_3. We find the pathway to be energetically feasible (−378 kcal/mol) once the initial CH_3S^- is available (this is our starting point). The overall activation barrier occurs at TS1 (2.8 kcal/mole above Ii). When we test the effect of using H_2O as the proton donor for the epoxide, a second much larger free energy barrier is found to occur between Ib and IVi, which would appear to vindicate the choice of a RSH as the donor and rule out H_2O as the donor. If there is no proton donor for the epoxide, the first two steps of the mechanism are largely unaffected, however the mechanism cannot proceed. It is likely that these structures will be very useful in a future QM/MM study of the enzymatic pathway once the enzyme structures are available. Studies like these are essential for ultimately understanding the details of controlled medical inhibition of VKOR through by medicinals such as Warfarin.

Acknowledgements

LGP is grateful to NIH for HL-06350 and to NSF for ITR/AT DMR-0121361. DWS is grateful to NIH for HL-48318. TW/DWD-II thank NIH/NCRR RR06009 for support. The authors thank the Pittsburgh Supercomputing Center and the UNC-CH Computing Center for computing resources.

Appendix A. Finding transition states for reactions between complex molecules

A.1. Rationale

Locating transition states can be a difficult process for complex systems of many atoms. We found, after considerable exploration, the following procedure to be effective. This procedure is keyed to the use of Gaussian03 [20] and Gaussview [23] but should be useful generally.

A.2. Definitions

$A(i) + B(j)$: A, B reacting molecules; i, j reacting atoms of A and B, respectively. $d(i, j)$ = distance between i and j. The geometry of starting (separated) complex is assumed to be established. ts = transition state (geometry).

A.3. Generally

It is important to view all starting, intermediate (including ts) and final structures carefully at each stage to visualize the chemistry happening.

1. Scan $d(i, j)$ using b3lyp/3-21g**, starting from $d(i, j)$ = large ∼4.0 Å. Use stepsize = 0.1 Å: opt = (modredundant, loose, maxcycle = 5000) scf = (fermi, conver = 5) . . . $i\,j$ 4.025 −0.1 (the minus insures stepping inward towards bond formation).
2. Find $d(i, j,$ near ts) on reactant side of scan by use of a view of the scan energy profile.
3. Using same method/basis set on $d(i, j,$ near ts) coords, do: opt = (ts, calcfc, noeigentest, maxstep = 5, loose) scf = (fermi, conver = 5) [if this procedure leads to expansion to reactants or products rather than ts, then redo steps (1,2) starting with $d(i, j,$ near ts) coords and a smaller stepsize. Find $d(i2, j2,$ near ts) and then repeat step 3] [if after repeating (1, 2, 3) and the potential ts still falls apart, then using $d(i2, j2,$ near ts), repeat step 3 with maxstep = 2].

4. If find ts optimization is successful [ts(low basis)], then optimize to the ts at the higher basis (6-311g**): opt = (ts, calcfc, noeigentest, maxstep = 5, loose) scf = (fermi, conver = 5).
5. If a ts is successfully found [ts(high basis)], remove the ''loose'' criteria from opt and scf and decrease the number of opt steps: opt = (ts, calcfc, noeigentest, maxstep = 2) to find ts(high basis, non-loose).
6. Determine the vibrational frequencies to confirm that a ts has been found opt = freq ... guess = check, geom = check [check = checkpoint file from 5].
7. If necessary (messy frequencies), repeat step 5 by adding ''tight'' to the opt list of options, and even possibly the separate option: integral = ultrafine to improve the grid upon which the dft electron density is computed. If energy differences are important, use of this last option will require that this option be used also for steps in energy difference calculations.

Appendix B. Supplementary data

Supplementary data associated with this article can be found, in the online version, at doi:10.1016/j.jmgm.2006.10.005.

References

[1] D.W. Stafford, The vitamin K cycle, J. Thromb. Haem. 3 (2005) 1873–1878.
[2] H. Dam, Haemorrhages in chicks reared on artificial diets: a new deficiency disease, Nature 133 (1934) 909–910.
[3] C. Vermeer, The Role of vitamin K in the post-translational modification of proteins, in: R.F.A. Zwaal, H.C. Hemker (Eds.), Blood Coagulation, Elsevier Publishers, Amsterdam, 1986, pp. 87–101.
[4] S.M. Wu, W.F. Cheung, D. Frazier, D.W. Stafford, Cloning and expression of the cDNA for human gamma-glutamyl carboxylase, Science 254 (1991) 1634–1636.
[5] S. Rost, A. Fregin, V. Ivaskevicius, E. Conzelmann, K. Hortnagel, H.J. Pelz, K. Lappegard, E. Seifried, I. Scharrer, E.G.D. Tuddenhham, C.R. Muller, T.M. Strom, J. Oldenburg, Mutations in VKORC1 cause warfarin resistance and multiple coagulation factor deficiency type 2, Nature 427 (2004) 537–541.
[6] T. Li, C.Y. Chang, D.Y. Jin, P.F. Lin, A. Khvorova, D.W. Stafford, Identification of the gene for vitamin K epoxide reductase, Nature 427 (2004) 541–544.
[7] J.E. Sadler, Medicine K is for koagulation, Nature 427 (2004) 493–494.
[8] H.A. Campbell, K.P. Link, Studies on the Hemorrhagic Sweet Clover Disease IV. The isolation and crystallization of the hemorrhagic agent, J. Biol. Chem. 138 (1941) 21–33.
[9] J.A. Last, The missing link: the story of Karl Paul Link, Toxicol. Sci. 66 (2002) 4–6.
[10] The top 200 generic drugs by unit in 2003. Drug Topics 148 (2004) 76 (news article).
[11] M.J. Rieder, A.P. Reiner, B.F. Gage, D.A. Nickerson, C.S. Eby, H.L. McLeod, D.K. Blough, K.E. Thummel, D.L. Veenstra, A.E. Rettie, Effect of VKORC1 haplotypes on transcriptional regulation and Warfarin dose, N. Eng. J. Med. 352 (2005) 2285–2293.
[12] L. Bodin, C. Verstuyft, D.A. Tregouet, A. Robert, L. Dubert, C. Funck-Brentano, P. Jaillon, P. Beaune, P. Laurent-Puig, L. Becquemont, M.A. Loriot, Cytochrome P450 2C9 (CYP2C9) and vitamin K epoxide reductase (VKORC1) genotypes as determinants of acenocoumarol sensitivity, Blood 106 (2005) 135–140.
[13] P. Dowd, R. Hershline, S.W. Ham, S. Naganathan, Vitamin K and energy transduction: a base strength amplification mechanism, Science 269 (1995) 1684–1691.
[14] P. Dowd, S.W. Ham, S. Naganathan, R. Hershline, The mechanism of action of vitamin K, Ann. Rev. Nutr. 15 (1995) 419–440.
[15] R.B. Silverman, Chemical model studies for the mechanism of vitamin K epoxide reductase, J. Am. Chem. Soc. 103 (1981) 5939–5941.
[16] R.B. Silverman, Vitamin K dependent carboxylation of proteins, in: The Organic Chemistry of Enzyme Catalyzed Reactions, Revised ed., Academic Press, London, 2002, pp. 298–303.
[17] L. Goodstadt, C.P. Ponting, Vitamin K epoxide reductase: homology, active site and catalytic mechanism, TIBS 29 (2004) 289–292.
[18] Y.J. Zheng, T.C. Bruice, Rapid enzyme-catalyzed heterolytic C–H bond cleavage by a base strength amplification mechanism: a theoretical examination of the mechanism of oxidation of vitamin K, J. Am. Chem. Soc. 120 (1998) 1623–1624.
[19] D.W. Deerfield II, C.H. Davis, T. Wymore, D.W. Stafford, L.G. Pedersen, Int. J. Quant. Chem. 106 (2006) 2944–2952.
[20] M.J. Frisch, G.W. Trucks, H.B. Schlegel, G.E. Scuseria, M.A. Robb, J.R. Cheeseman, J.A. Montgomery Jr., T. Vreven, K.N. Kudin, J.C. Burant, J.M. Millam, S.S. Iyengar, J. Tomasi, V. Barone, B. Mennucci, M. Cossi, G. Scalmani, N. Rega, G.A. Petersson, H. Nakatsuji, M. Hada, M. Ehara, K. Toyota, R. Fukuda, J. Hasegawa, M. Ishida, T. Nakajima, Y. Honda, O. Kitao, H. Nakai, M. Klene, X. Li, J.E. Knox, H.P. Hratchian, J.B. Cross, C. Adamo, J. Jaramillo, R. Gomperts, R.E. Stratmann, O. Yazyev, A.J. Austin, R. Cammi, C. Pomelli, J.W. Ochterski, P.Y. Ayala, K. Morokuma, G.A. Voth, P. Salvador, J.J. Dannenberg, V.G. Zakrzewski, S. Dapprich, A.D. Daniels, M.C. Strain, O. Farkas, D.K. Malick, A.D. Rabuck, K. Raghavachari, J.B. Foresman, J.V. Ortiz, Q. Cui, A.G. Baboul, S. Clifford, J. Cioslowski, B.B. Stefanov, G. Liu, A. Liashenko, P. Piskorz, I. Komaromi, R.L. Martin, D.J. Fox, T. Keith, M.A. Al-Laham, C.Y. Peng, A. Nanayakkara, M. Challacombe, P.M.W. Gill, B. Johnson, W. Chen, M.W. Wong, C. Gonzalez, J.A. Pople, Gaussian 03, Revision C.02, Gaussian Inc., Wallingford, CT, 2004.
[21] C.T. Lee, W.T. Yang, R.G. Parr, Development of the Colle–Salvetti correlation-energy formula into a functional of the electron density, Phys. Rev. B 37 (1998) 785–789.
[22] R. Krishnan, J.S. Binkley, R. Seeger, J.A. Pople, Self-consistent molecular orbital methods XX. A basis set for correlated wave functions, J. Chem. Phys. 72 (1980) 650–654.
[23] Gaussview, Gaussian Inc., Carnegie, PA, 2003.
[24] Y.H. Ding, Z.S. Li, Y.G. Tao, X.R. Huang, C.C. Sun, Theoretical study on structures and stability of HC2P isomers, Theor. Chem. Acc. 107 (2002) 253–265.
[25] L.T. Chen, H.M. Xiao, J.J. Xiao, DFT study of the mechanism of nitration of toluene with nitronium, J. Phys. Org. Chem. 18 (2005) 62–68.
[26] H.H. Thijssen, Y.P. Janssen, L.T. Vervoort, Microsomal lipoamide reductase provides vitamin K epoxide reductase with reducing equivalents, Biochem. J. 297 (1994) 277–280.
[27] J.K. Tie, C. Nicchitta, G. Heijne, D.W. Stafford, Membrane topology mapping of vitamin K epoxide reductase by in vitro translation/cotranslation, J. Biol. Chem. 280 (2005) 16410–16416.
[28] N. Wajih, D.C. Sane, S.M. Hutson, R. Wallin, Engineering of a recombinant vitamin K-dependent γ-carboxylation system with enhanced γ-carboxyglutamic acid forming capacity: evidence for a functional CXXC redox center in the system, J. Biol. Chem. 280 (2005) 10540–10547.